Supporting Information

STORM as a Tool to Track Cargo Release from Polymeric Nanocarriers at the Single-Particle Level

Anna Solé-Porta*, Sílvia Pujals*, Pietro Delcanale, Anna Roig*

Anna Solé-Porta, Anna Roig
Institut de Ciència de Materials de Barcelona (ICMAB-CSIC), Campus UAB, 08193 Bellaterra, Spain
E-mail: asole@icmab.es, roig@icmab.es

Sílvia Pujals
Department of Biological Chemistry, Institute for Advanced Chemistry of Catalonia (IQAC-CSIC), 08034 Barcelona, Spain
E-mail: silvia.pujals@iqac.csic.es

Pietro Delcanale
Department of Mathematical, Physical and Computer Sciences, University of Parma, 43124 Parma, Italy

Materials and methods

Materials: PLGA (Resomer® RG 502 H, acid-terminated, lactide:glycolide 50:50, MW=7-17 kDa), polyvinyl alcohol (87-90% hydrolyzed, MW=30-70 kDa), triethylamine (≥99.5%), β-mercaptoethylamine, Oxyrase, and sodium DL-lactate were purchased from Sigma-Aldrich. D(+)-trehalose 2-hydrate was purchased from AppliChem Panreac and Cyanine5-NHS ester (Cy5, 95%) from Lumiprobe. Bovine serum albumin Alexa Fluor 488 conjugate (BSA-AF488) and TetraSpeck™ microspheres (0.1 µm, fluorescent blue/green/orange/dark red) were purchased from Life Technologies. Ultrapure water was produced using a Milli-Q Advantage A10 system from Millipore. All other chemicals and reagents were of the highest purity grade commercially available.

Synthesis of PLGA-Cy5/BSA-AF488 NCs: PLGA-Cy5 NCs loaded with BSA-AF488 (PLGA-Cy5/BSA-AF488 NCs) were prepared using the double emulsion-solvent evaporation method.[1,2] An aqueous solution of 80 % w/w non-fluorescent BSA and 20% w/w fluorescent BSA-AF488 was prepared to a final protein concentration of 20 mg mL^{-1} (50 µL). This first aqueous phase (w_1) was added to 500 µL of dichloromethane (DCM), which is the organic phase (o). The latter contained 49.5 mg of unlabeled PLGA and 0.5 mg of PLGA-Cy5 (1% w/w), synthesized as in previous works.[3–5] A first emulsification was done by sonicating at 200 W for 28 s to form a water-in-oil emulsion (w_1/o). Then, an aqueous polyvinyl alcohol solution (2 mL, 20 mg mL^{-1}), which is the external aqueous phase (w_2) and acts as a stabilizer, was added, and a water-in-oil-in-water emulsion (w_1/o/w_2) was formed by sonicating again at 200 W for 28 s. During the emulsion process, the temperature was kept at 4 °C using an ice bath.

The resulting double emulsion was poured into 50 mL of ultrapure water (MilliQ) and mechanically stirred at 280 rpm at rt for 2 h in dark conditions. Then, the NCs were purified by centrifugation in ultrapure water at 4 °C. Centrifugation was performed at 943 g for 15 min, followed by two centrifugations at 9435 g for 15 min. The NCs were finally redispersed in 6 mL of a 2 mg mL^{-1} trehalose aqueous solution, acting as a cryoprotectant. The solution was frozen at –80 °C for a posterior lyophilization process (LyoMicron –85 °C, Coolvacuum) for 72 h to preserve the NCs from hydrolytic degradation. The as-obtained NCs in a powder form were stored at –80 °C until their use. The stability of the lyophilized PLGA NCs is ensured during 2 months of cryo-storage, as shown in a previous study.[6]

Fluorescent PLGA-Cy5 NCs with non-fluorescent BSA and non-fluorescent PLGA NCs with fluorescent BSA-AF488 were also synthesized to be used as controls.

Cryo-TEM: Cryo-TEM samples were prepared onto glow-discharged holey carbon grids (C-flat™). NCs suspensions in water were diluted to a final concentration of 2 mg mL^{-1} and 3 µL of the sample were added to the grid, blotted for 3 s and vitrified in liquid ethane using a Vitrobot Mark IV plunging system (Thermo Fisher Scientific). Cryo-TEM grids were stored at liquid nitrogen temperature.

NCs were imaged at the Joint Electron Microscopy Center (JEMCA) at the ALBA synchrotron (Cerdanyola del Vallès, Spain) using a 200 kV Glacios TEM equipped with extreme field emission gun

(X-FEG) optics, a cryogenic sample manipulator robot for up to 12 grids, and a Falcon 4 direct electron detector (Thermo Fisher Scientific). Images were analyzed using the Velox software.

STEM-EDX: NCs suspensions were prepared in water at 2 mg mL^{-1} and one drop was dried on Lacey Carbon grids at rt. The composition of the NCs was investigated by energy-dispersive X-ray spectroscopy in a STEM at the JEMCA at the ALBA synchrotron (Cerdanyola del Vallès, Spain) on a double-corrected ThermoFisher Spectra 300 (S)TEM microscope operated at 60 kV. EDX spectra were acquired using a four quadrant Super-X windowless silicon drift detector system. The images and spectra were analyzed using the Velox software.

SEM: A field-emitting scanning electron microscope (SEM, FEI Quanta 200 FEG) was used to study the morphology of the NCs. The samples at the different release time points were diluted to 0.1 mg mL^{-1} using ultrapure water, and 10 µL of the slightly turbid suspension was placed onto a small piece of a silicon wafer stuck on the top of a carbon layer. The sample was dried at rt overnight and then sputtered with 60/40 Au/Pd (20 mA for 2 min to have 10 nm deposition) with an Emitech K550 instrument (Quorum Technologies Ltd.). Secondary electron images were taken using a working distance of 8 mm, a large field detector, an acceleration voltage of 15 kV, and a pressure of 60 Pa.

NTA: NTA was performed with a Nanosight NS300 (Malvern Instruments, Malvern, UK) equipped with a 488 nm laser to obtain the hydrodynamic diameter and the concentration of NCs. All suspensions were diluted to 0.1 mg mL^{-1} in ultrapure water and loaded into the sample chamber. The scattered light was visualized by a 20× magnification microscope equipped with a sCMOS (scientific Complementary Metal Oxide Semiconductor) camera, which allowed us to record real-time videos. Measurements were performed in triplicate. Automatic data analysis was performed on recorded data using the NTA 3.4 software.

In vitro release experiment: The release experiment was performed by incubating PLGA-Cy5/BSA-AF488 NCs at 37 °C in PBS 1X (pH=7.4) at a concentration of 5 mg mL^{-1} of NCs. At specific time points (0 h, 1 h, 12 h, 1 day, 4 days, 16 days, and 30 days), 50 µL of the NCs suspension were retrieved and stored at –80 °C until STORM imaging. No other purification step that could potentially damage the nanocarriers was performed.

STORM sample preparation and imaging: To perform dSTORM imaging, 40 µL of NCs suspensions (0.4 mg mL^{-1}) at different time points were immobilized by adsorption onto the surface of a flow chamber assembled using a glass slide and a coverslip (24 mm × 24 mm, thickness 0.15 mm) separated by double-sided tape. After being incubated for 5 min upside down, 100 µL of fiducial markers (TetraSpeck microspheres, 1:500 dilution) were added and immobilized by adsorption for 5 min onto the surface to correct the lateral mechanical drift during acquisition. Finally, 60 µL of the dSTORM buffer (OxEA) was added, which contains 39 µL of PBS 1X pH=8.4, 6.3 µL of 100 mM β-mercaptoethylamine (MEA), and an oxygen scavenging system composed of 12.7 µL of 20% (v/v)

sodium DL-lactate and 2 µL of 3% (v/v) Oxyrase to eliminate the oxygen radicals.[7] A diagram of the experimental procedure can be seen in **Scheme S1**.

Five dSTORM images were acquired for each time point using a Nikon N-STORM microscope configured for total internal reflection fluorescence imaging and endowed with Perfect Focus system to prevent z-drift. Cy5-labeled NCs were imaged using the 647 nm laser (160 mW), and BSA-AF488 was imaged through the 488 nm laser (80 mW). Fiducial markers were imaged by the 561 nm laser (80 mW). No UV light activation was employed. Fluorescence was collected using a Nikon 100×, 1.49 NA oil immersion objective and passed through a quad-band-pass dichroic filter (97335 Nikon). Images were acquired over a 256 × 256 pixel region (pixel size 0.16 µm) using a Hamamatsu ORCA-Flash 4.0 camera with a 10 ms exposure time. 20,000 frames were acquired for channel 647 first, followed by 20,000 frames for channel 488, and the total time required to acquire one image was about 10 min. One frame for channel 561 (drift correction) was acquired every 100 frames. Control dSTORM images were performed by recording images of fluorescent NCs with non-fluorescent protein and non-fluorescent NCs with fluorescent BSA to discard cross-channel blinking artifacts (**Figure S11**). Before measurements, the channels were aligned using TetraSpeck beads to correct for residual chromatic aberrations.

STORM data analysis: dSTORM images were analyzed using the STORM module of the NIS Element Nikon software, which generates a list of localizations by Gaussian fitting of blinking dyes in the acquired movies. Blinkings detected in consecutive frames were counted as a single blinking event by the software to prevent overestimation. The thresholds for the 647 and 488 channels were set to 500 and 250, respectively. No additional filters were applied. Then, the lists of localizations (.txt file) obtained with NIS-Elements were further processed using a MATLAB code specifically upgraded from Delcanale *et al* to obtain quantitative information about the protein release from the PLGA nanocarriers.[8]

Firstly, the text file generated by NIS-Elements was scanned by the function *ReadCoords3.m* to extract the position and time (XYT) coordinates for the three different channels: nanocarrier (647), protein (488) and fiducial markers (561), used for drift correction. The XYT coordinates were further analyzed using the *Cluster2_quantification.m* code, schematically explained in **Figure 2**, which first reads the three channels' coordinates and then plots the raw XY localizations. To roughly identify the centers of valid nanocarriers and fiducial markers, the code performed a mean-shift clustering on both channels after setting a specific bandwidth (50 nm). This is the key parameter that determines clustering and is usually set to the half-radius of the nanoparticles (nm). This value provided an optimal balance between minimizing nanoparticle fragmentation and enabling the discrimination of adjacent nanocarriers. After the identification of the centers of nanocarriers and fiducial markers, the nanocarrier channel was filtered by different criteria: 1) the number of localizations (*MinPts*: the NCs with less than 20 localizations were not considered), 2) the diameter (*MaxDiam*: the NCs with a diameter larger than 200 nm were excluded), 3) the aggregation distance (*MinClustDist*: the NCs closer than 50 nm to each other were discarded), 4) the elongation (*Elong*: the NCs with a long:short axis

ratio of fitted ellipse larger than 10 were not counted), and 5) the distance to fiducial marker (*DistFidRef*: the clusters identified as NCs but closer than 100 nm to a fiducial marker were discarded to avoid false positives). After this filtering, a size check enabled robust determination of the center and radius of each nanocarrier based on its localizations. Examples of discarded NCs are shown in **Figure S12**.

Finally, the protein localizations associated with each nanocarrier were identified as non released. For that, we considered protein localizations within the nanocarrier's radius or very close to it (within 30% of the radius). Therefore, for each particle, we defined a circumference with a radius equal to the particle's radius multiplied by a factor (*Factor*=1.3), which was set after trial-and-error tests to provide a safety margin. Given the dynamic nature of polymeric nanocarriers, accounting for this factor was necessary to capture the NCs' morphological transformation.

The scripts used for the analysis are publicly available on a GitHub repository (https://github.com/annasoleporta/STORM_release_analysis). The repository includes detailed documentation of the workflow and example datasets to facilitate testing and reproduction of the analysis.

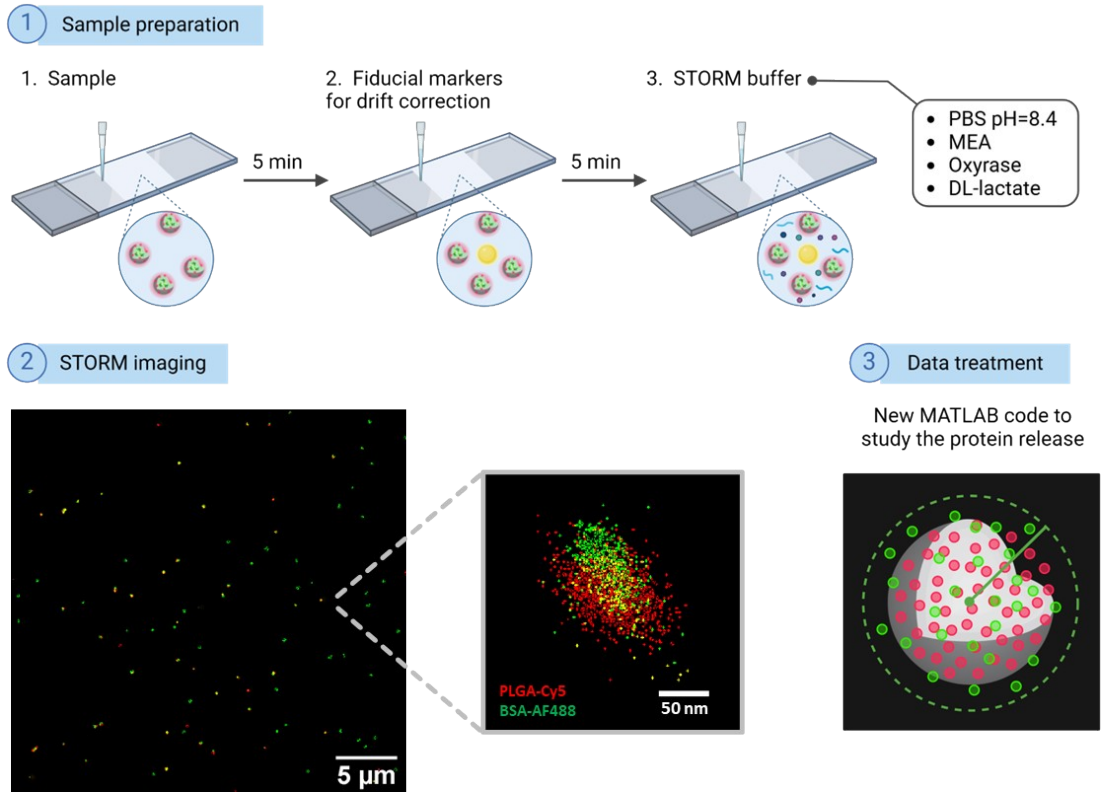

Scheme S1. Methodology followed for the study of protein release by dSTORM. 1) Sample preparation: first, 40 µL of a NCs suspension (0.4 mg mL^{-1}) was injected into a flow chamber assembled using a glass slide and a coverslip with double-sided tape. After 5 min deposition upside down, 100 µL of fiducial markers (1:500) were added. After an additional 5 min, 60 µL of dSTORM buffer was added, containing PBS 1X at pH=8.4, β-mercaptoethylamine (MEA), Oxyrase, and DL-lactate. 2) dSTORM imaging. 3) Data treatment with a MATLAB code, allowing us to perform protein release analysis.

Validation of analysis parameters for nanocarrier identification and protein release quantification: To validate the key parameter to define protein release, the nanocarrier identification, based on the parameters *MinPts, MaxDiam, MinClustDist, Elong, DistFidRef,* was first optimized using data from the initial time point (0 h), when nanocarrier integrity is complete. Parameter selection was based on nanocarrier's characteristics and performed via systematic testing of a range of values, followed by careful visual inspection to ensure accurate NC identification while minimizing false positives and misassignments. Details of the ranges tested for each values are described below:

- To know the minimum number of Cy5 localizations to consider a nanocarrier (*MinPts*), values of 10, 20, 30, and 50 were evaluated. A value of 20 was selected as an optimal compromise between reducing false detections arising from background localizations and maintaining sensitivity to detect partially degraded NCs at later time points, where fewer Cy5 localizations were present.
- To evaluate the nanocarrier diameter (*MaxDiam*), values of 100, 150, 200, and 300 nm were tested. A threshold of 200 nm was chosen to ensure selection of larger NCs, which may encapsulate higher protein loads and therefore influence the release behaviour.
- To determine the minimum distance between clusters to be considered isolated (*MinClustDist*), values of 50, 100, 200, and 300 nm were tested. A value of 50 nm was selected based on NC size, meaning that any valid NC whose centre of mass was closer than 50 nm to the centre of mass of another valid NC was excluded to prevent misassignment of protein localizations.
- Elongation parameter (*Elong*): values of 1, 10, and 20 were tested. A value of 10 was selected to account for some spherical geometry deviation due to synthesis, experimental variability, and incomplete drift correction.
- Distance to fiducial markers (*DistFidRef*): values of 80, 100, and 120 nm were explored. A value of 100 nm was selected based on careful case-by-case inspection to effectively exclude false positives arising from fiducial markers blinking in the reference channel.

Regarding the quantification of the protein, the code was originally developed to account for protein localizations at a fixed distance from the nanocarrier centre, regardless of the NC size at different time points. However, in the improved code, protein localization selection was defined relative to each individual nanocarrier by introducing a size-dependent proximity criterion. To evaluate the robustness of this parameter and address concerns about arbitrariness, we analyzed multiple values of *FactorMaxDist* (1.1, 1.3, 1.5). A value of 1.3 was selected to account for the different precision of dSTORM in the two colours, especially for small radii nanoparticles. Importantly, the quantitative results of protein/NC were not significantly affected by the choice of this parameter within this range. Statistical analysis using the non-parametric Kruskall-Wallis ANOVA test followed by Dunn's multiple comparison test confirmed that no significant differences were observed between the tested conditions, as seen in the **Figure S13**. These results demonstrate that the release quantification is robust to moderate and rational variations in the proximity threshold.

Calibration of AF488 localizations per protein molecule: To achieve a quantitative estimation of the number of protein molecules per nanocarrier, it is necessary to consider the multiple localizations that can originate from a single dye (AF488) due to blinking during STORM acquisition. To account for this effect, a calibration was performed to estimate the statistical distribution of these blinking events, as in Feiner-Gracia *et al*.[9] Since this phenomenon strongly depends on the environment, reference

measurements were performed under the same acquisition conditions (buffer, laser power, exposure time, frames) as the main experiments. This calibration is based on the rationale that the number of localizations is proportional to the number of labelled molecules, and it provides useful estimated values.

A 100 pg/mL BSA-AF488 suspension in PBS 1X (pH=7.4) was prepared to image individual protein molecules. At this concentration, protein localizations appeared as clearly isolated clusters enabling direct quantitative analysis. Three different images obtained for this experiment were analyzed using the NIS-Elements Nikon software configured with identical settings to those used in the main experiments. The resulting localization dataset was exported and analyzed in MATLAB using a mean-shift clustering algorithm, with a bandwidth of 100 nm, sufficient to avoid merging signals coming from different proteins. Cluster centers corresponding to individual proteins were then filtered according to the following criteria: 1) *MinPts*=5 localizations, 2) *MaxDiam*=50 nm, 3) *MinClustDist*=50 nm, and 4) *Elong*=10.

Then, a histogram of the number of localizations per single protein was constructed. Given that fluorophore blinking follows a geometric distribution,[10,11] the number of localizations per single protein was estimated as the median of a decaying exponential function fitted to this histogram (**Figure S8**). Finally, the number of proteins associated with each nanocarrier was estimated by dividing the median number of protein localizations assigned to that nanocarrier by the corresponding median number of localizations per single protein derived from the calibration measurements.

Fluorophore stability assessment: The stability of Cy5 and AF488 within the nanocarrier formulations was evaluated by monitoring their spectroscopic properties over time (**Figure S10**). For Cy5, PLGA nanocarriers labelled with 50% Cy5 were used to ensure sufficient signal intensity for quantitative measurements. Absorbance spectra of nanocarriers suspensions (0.5 mg mL^{-1} in PBS 1X) were recorded at specific time points (0 and 30 days) using a Jasco V-780 UV-vis spectrophotometer, and changes in the characteristic Cy5 absorption band were analyzed.

The stability of AF488 was assessed by recording fluorescence emission spectra of PLGA-Cy5/BSA-AF488 nanocarriers at 1 h and 30 days (5 mg mL^{-1} in PBS 1X) using a Tecan Spark microplate reader. Samples were excited at 485 nm, and emission spectra were compared to evaluate potential changes in band position or intensity over time.

Statistical analysis: All data were analyzed using Origin 2024b and GraphPad Prism 9.2 software.

Nanocarrier size and concentration data are reported as mean ± standard deviation (SD), and comparisons among more than two groups were performed using one-way ANOVA followed by Tukey's multiple comparison test.

For protein release measurements, distribution fitting was performed using multiple candidate models (normal, lognormal, Weibull, gamma, and exponential), and goodness-of-fit was evaluated using the Kolmogorov-Smirnov test. Among these, the gamma distribution provided the best fit to the

data, indicating deviations from normality. Since protein localization events exhibited skewed distributions, central tendency was described using the median rather than the mean. Therefore, these data are reported as median ± median absolute deviation (MAD). Statistical comparisons were performed using the non-parametric Kruskal-Wallis test followed by Dunn's multiple comparison test. In all cases, $P < 0.05$ was considered statistically significant.

Supplementary Figures

Figure S1. Cryo-TEM images of representative empty and protein-loaded PLGA NCs and their corresponding intensity profiles. (a) Empty PLGA NCs and b) BSA-loaded PLGA NCs with the corresponding profile. c) Averaged intensity profiles (normalized and smoothed) obtained from cryo-TEM images of empty PLGA NCs (N=6, in grey) and BSA-loaded PLGA NCs (N=6, in orange). The decrease in the intensity is higher for BSA-loaded NCs, indicating the presence of protein in their inner core.

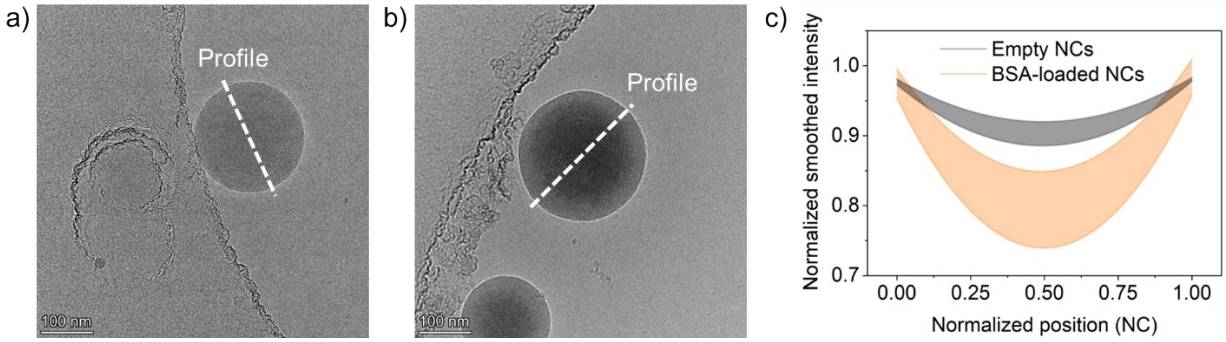

Figure S2. Elemental quantification by EDX, showing the absence of nitrogen band for empty PLGA NC and the visible nitrogen band from the amino groups in the amino acid residues of the protein in the BSA-loaded NCs.

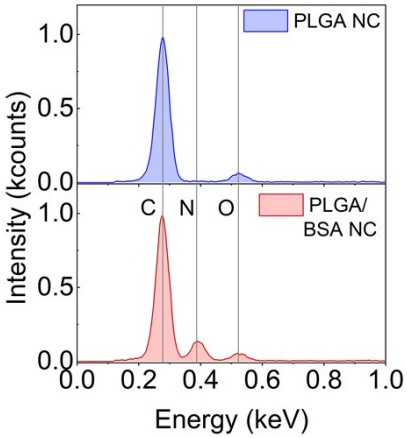

Figure S3. Intensity hydrodynamic size distribution of PLGA-Cy5/BSA-AF488 NCs and their Z-potential value measured by dynamic light scattering.

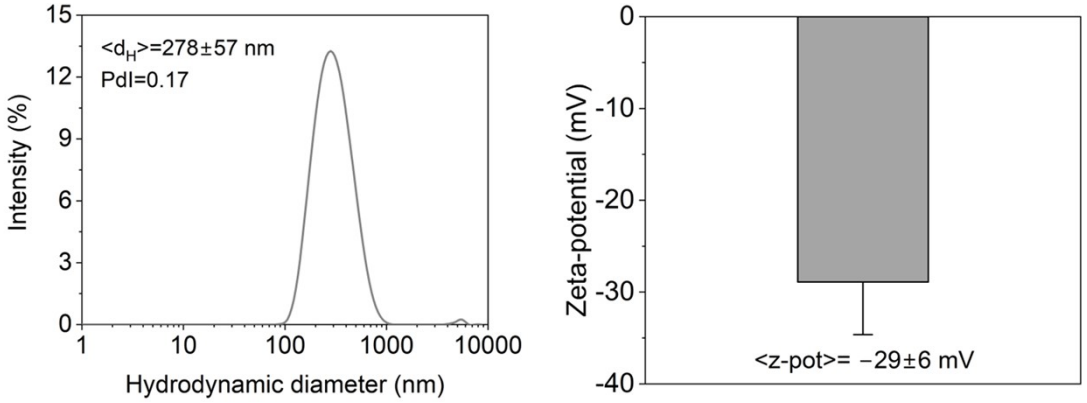

Table S1. Descriptive statistics of the nanocarrier diameter at different time points obtained by dSTORM. For each time point, the number of analyzed nanocarriers (N), mean, standard deviation, median, interquartile range (IQR), and median absolute deviation (MAD) are reported.

Time point	N	Mean	Standard deviation	Median	Interquartile Range (IQR)	Median absolute deviation (MAD)
0h	594	69	27	64	34	16
1h	1663	79	25	78	32	16
12h	1712	68	21	64	20	10
1d	2843	76	20	72	22	10
4d	524	69	19	64	21	10
16d	236	97	21	94	24	12
30d	30	108	41	113	60	29

Figure S4. Diameter distributions of nanocarriers at different time points: a) obtained by dSTORM, shown as histograms with lognormal fits. For each time, the number of analyzed nanocarriers (N), the mean ± standard deviation, and the median are reported; b) obtained by NTA. The standard deviation is shown in a lighter color (N=3).

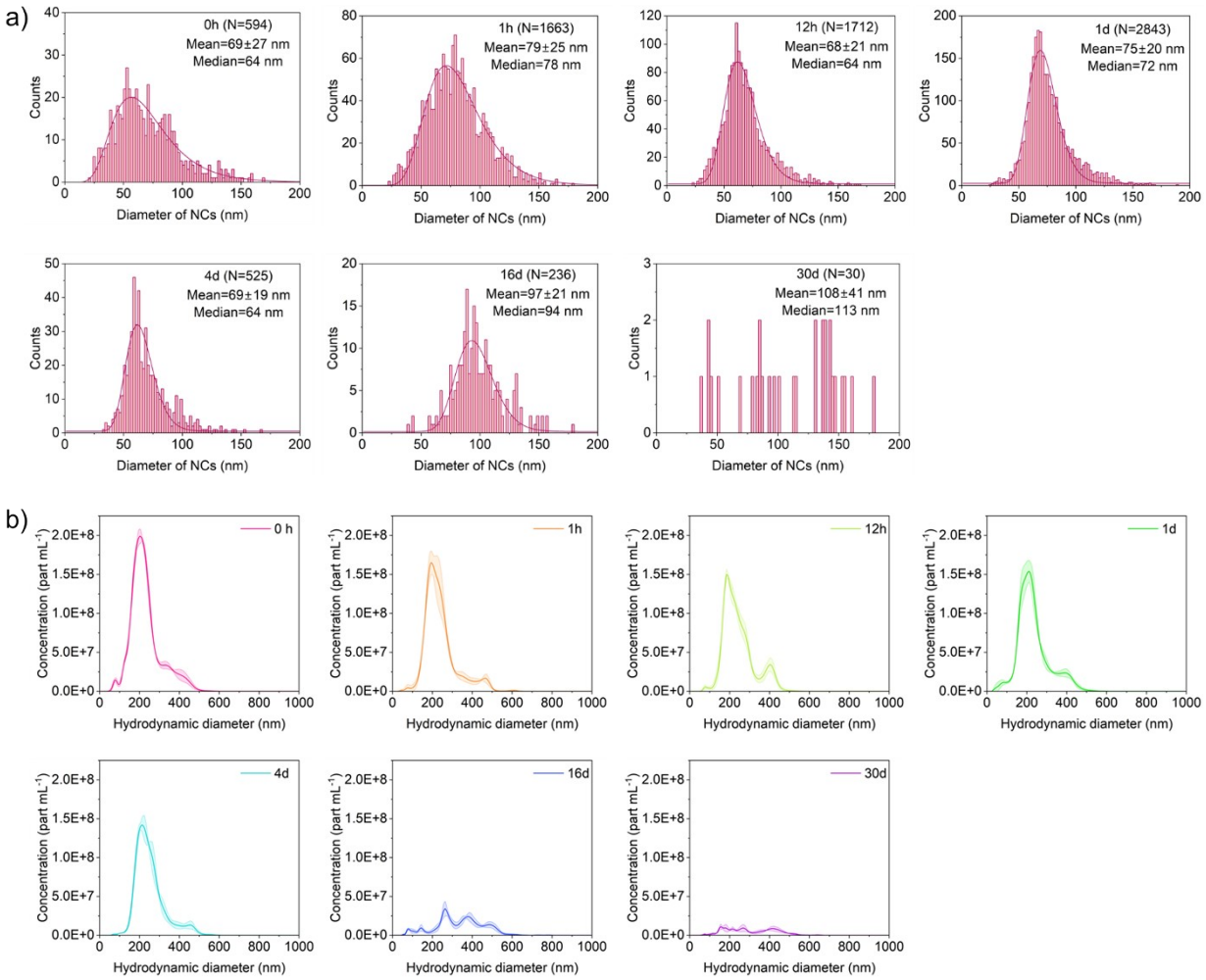

Figure S5. Histograms of the number of Cy5 localizations obtained by dSTORM, showing the relative frequency together with the median (vertical dashed line).

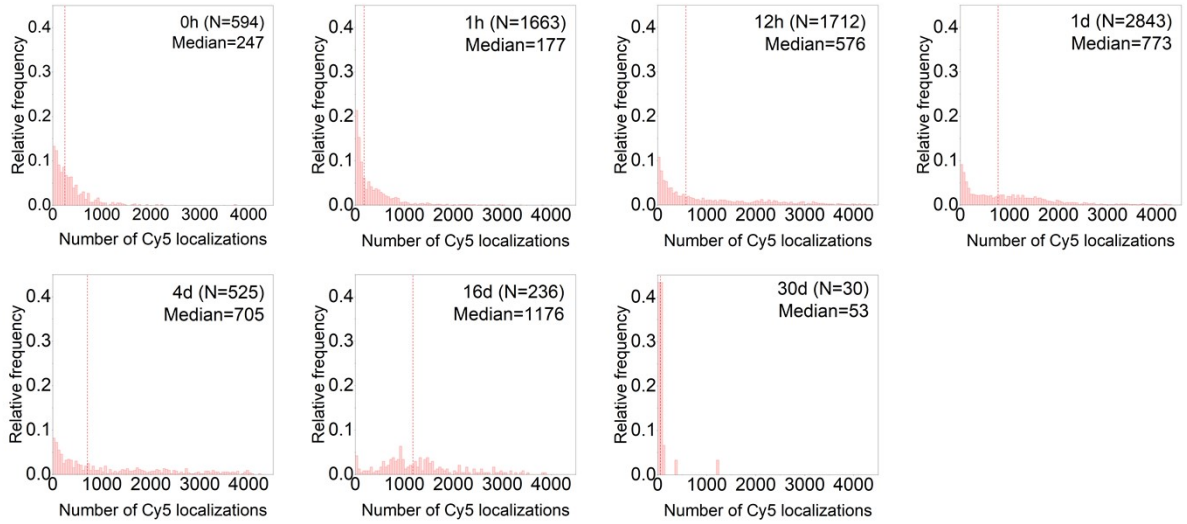

Table S2. Descriptive statistics of the number of protein localizations per nanocarrier at different time points during the release experiment obtained by dSTORM. For each time point, the number of analyzed nanocarriers (N), mean, standard deviation, median, interquartile range (IQR), and median absolute deviation (MAD) are reported.

Time point	N	Mean	Standard deviation	Median	Interquartile Range (IQR)	Median absolute deviation (MAD)
0h	70	158	153	98	115	48
1h	90	182	201	105	189	70
12h	97	171	244	77	142	57
1d	112	167	113	155	204	100
4d	73	68	81	40	78	32
16d	65	61	73	26	92	25
30d	14	43	69	0	84	0

Figure S6. Histograms of the number of protein localizations per NC at different time points. The green solid line represents the gamma distribution fit, identified as the best model based on Kolmogorov-Smirnov goodness-of-fit test. The number of NCs analyzed (N), the median, and the median absolute deviation (MAD) are reported.

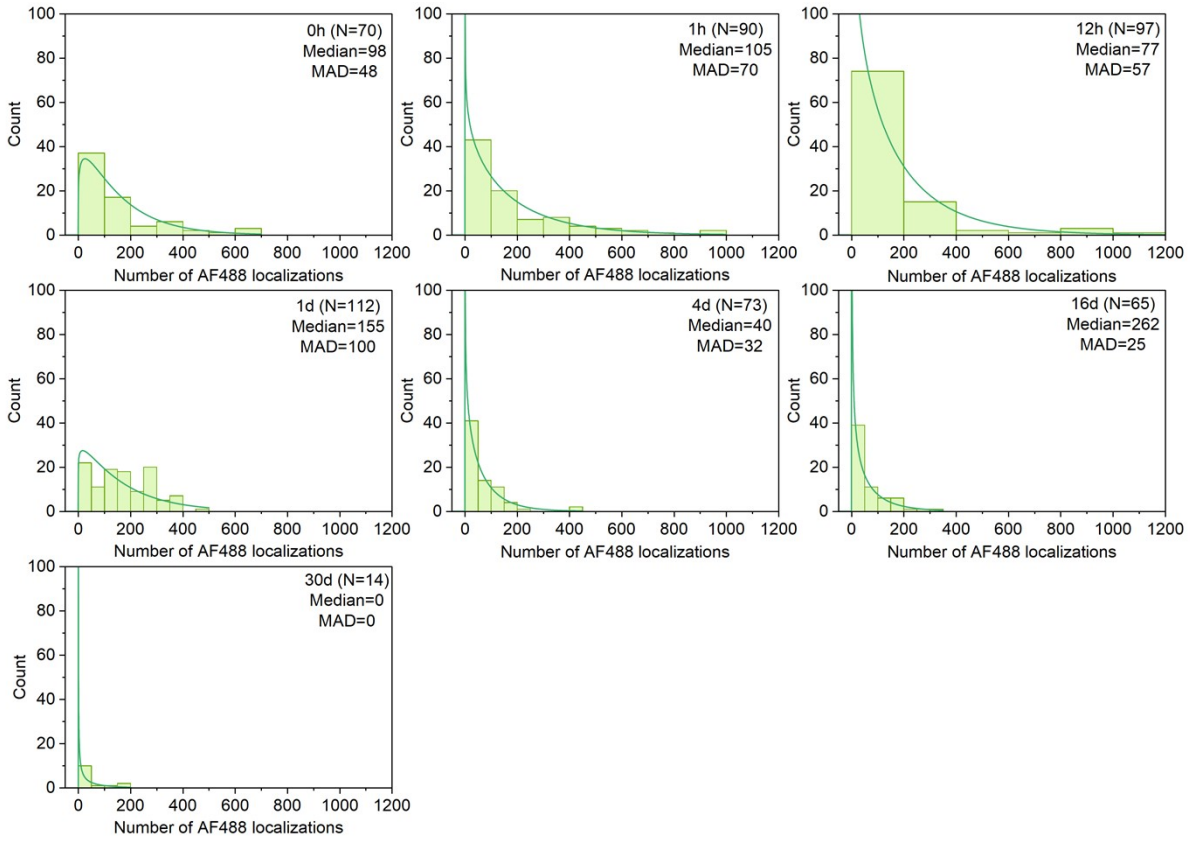

Figure S7. Box plot showing the distribution of protein localizations per nanocarrier at different time points. The horizontal line represents the median, the cross indicates the mean, the box corresponds to the interquartile range (IQR), and the whiskers denote the range excluding outliers. Adjacent to each box, the corresponding fitted gamma distribution illustrates the probability density of protein localizations per nanocarrier. This representation reveals substantial variability between nanocarriers within each time point, evidencing the heterogeneous nature of protein encapsulation within the PLGA NC population.

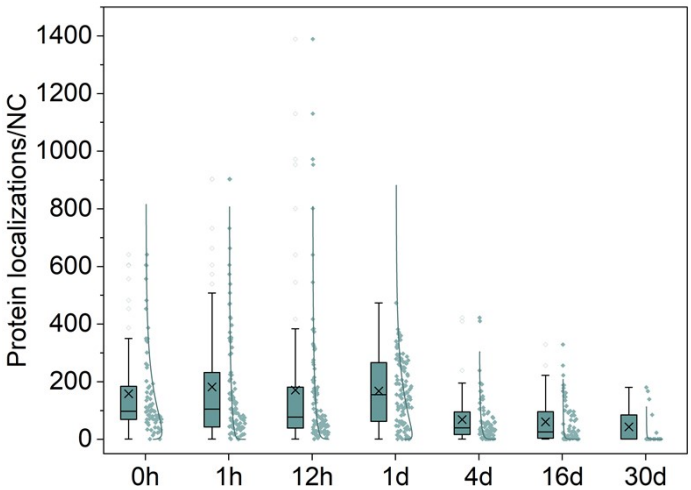

Figure S8. Distribution of AF488 localizations per BSA molecule. a) Histograms of the number of localizations per single protein molecule due to blinking. The green dashed line represents the exponential fit and the vertical gray dashed line indicates the median of the distribution. For this experiment STORM images are acquired in the same imaging conditions as during the main experiments. b) Box-and-whisker plot showing the mean (×), median (line), and the interquartile range (IQR, box). The points beyond the whiskers are considered outliers.

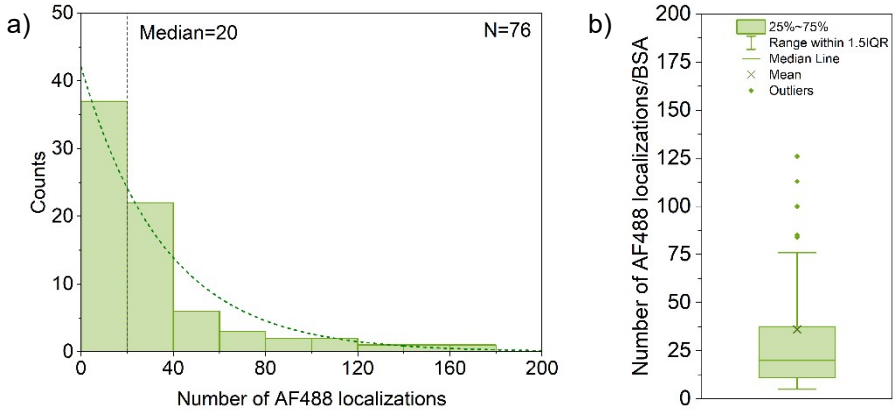

Figure S9. Comparison of protein release from PLGA nanocarriers measured by the Bradford assay (bulk analysis) and dSTORM (single-particle analysis), both exhibiting a similar biphasic profile characterized by an initial burst phase followed by sustained release. Plot shows cumulative percentage of released protein over time. Error bars of Bradford data points show the standard deviation. Error bars of dSTORM data are not shown for graph clarity.

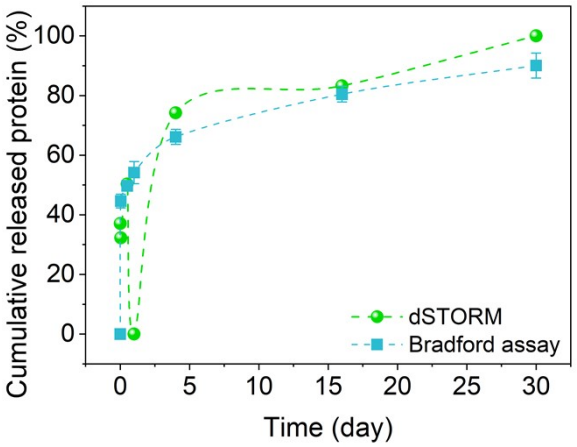

Figure S10. Fluorophore stability over time. a) Absorbance spectra of PLGA-Cy5 nanocarriers recorded at 0 and 30 days. The main absorption band remains centered at 650 nm at all time points, with only 5% decrease in absorbance after 30 days relative to the initial point, indicating minimal photophysical degradation of the Cy5 moiety. b) Fluorescence emission spectra of PLGA-Cy5/BSA-AF488 measured at the beginning of the release experiment (1 hour) and after 30 days. In both cases, the emission bands of AF488 are centered at 528 nm and their intensities are comparable, confirming fluorophore stability over time. The excitation wavelength (λ_{exc}) was set to 485 nm.

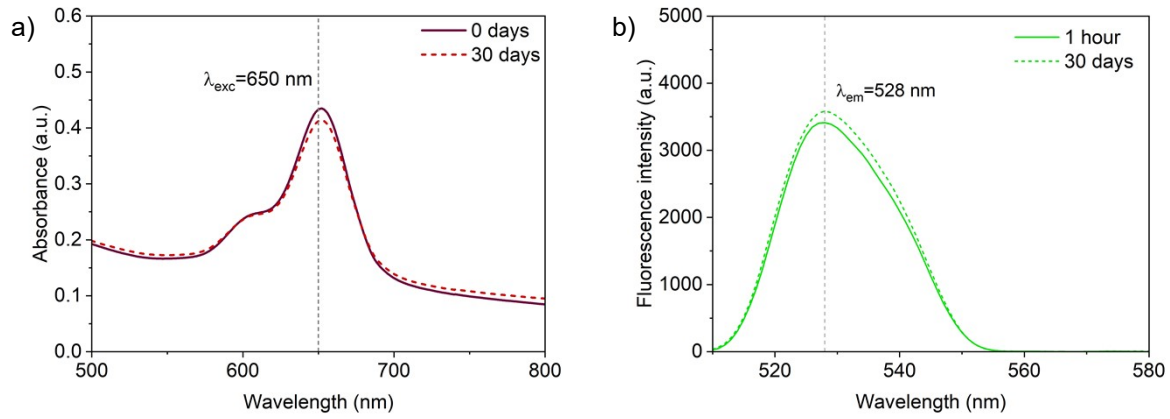

Figure S11. Control dSTORM images performed to discard cross-channel blinking artifacts. a) dSTORM image of PLGA-Cy5 nanocarriers without fluorescent protein. Red clusters correspond to nanocarriers detected in the 647 nm channel, while only a few isolated green localizations appear in the 488 nm channel due to background noise. b) dSTORM image of PLGA/BSA-AF488 nanocarriers without Cy5 labeling. Green clusters correspond to protein molecules detected in the 488 nm channel, with negligible red Cy5 localizations in the 647 nm channel, confirming the absence of crosstalk.

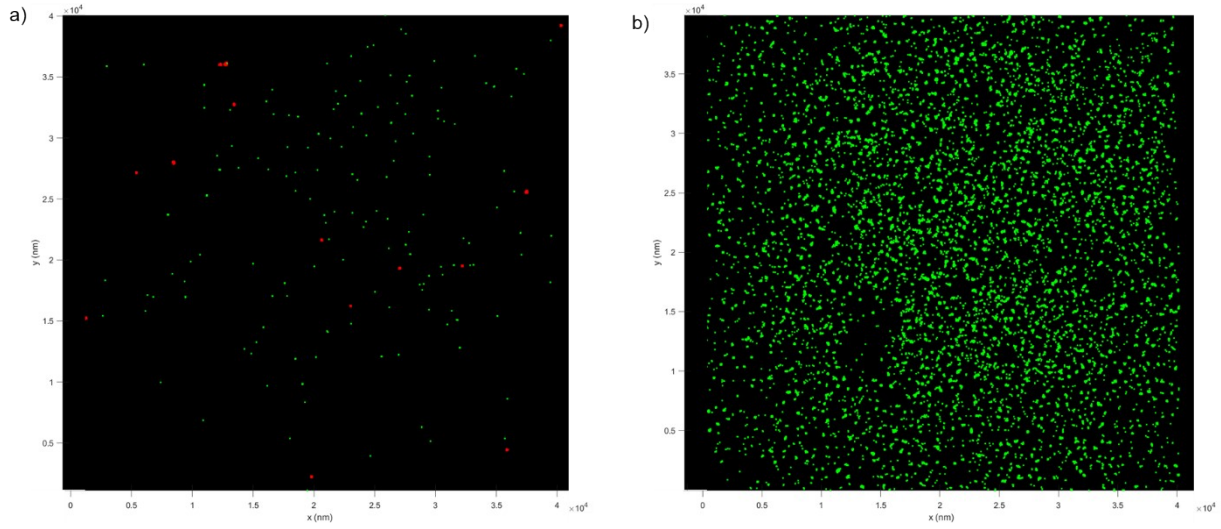

Figure S12. Examples of discarded nanocapsules in the protein release study by dSTORM due to the clear mismatch between PLGA-Cy5 and a large number of BSA-AF488 localizations, probably caused by an incorrect drift correction.

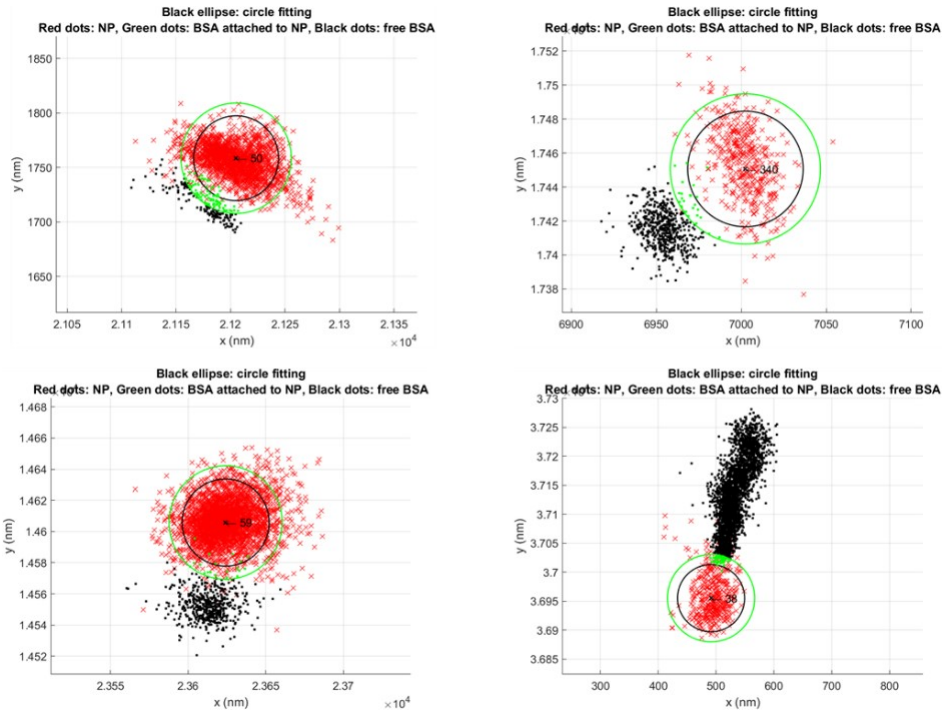

Figure S13. Protein localizations per nanocarrier at different time points using three values of the scaling factor (*FactorMaxDist*=1.1, 1.3, and 1.5). Box plots represent the median (line), the mean (cross), and interquartile range (IQR, box). No statistically significant differences were observed between the tested conditions (Kruskal-Wallis test followed by Dunn's multiple comparison test).

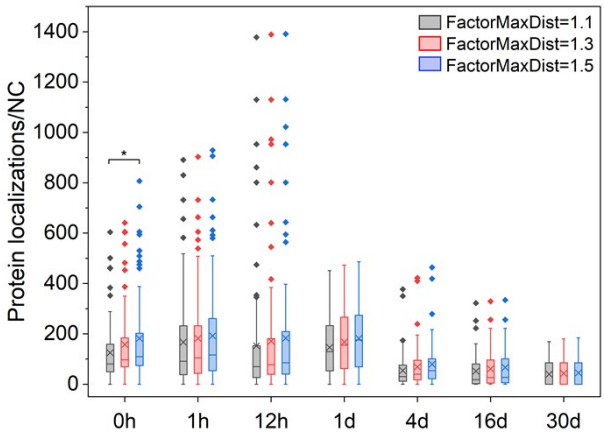

References

1 A. Solé-Porta, A. Areny-Balagueró, M. Camprubí-Rimblas, E. Fernández Fernández, A. O'Sullivan, R. Giannoccari, R. MacLoughlin, D. Closa, A. Artigas and A. Roig, *Small Sci.*, 2024, **4**, 2400066.

2 Y. Zhang, M. García-Gabilondo, A. Rosell and A. Roig, *Pharmaceutics*, 2019, **12**, 16.

3 Y. Zhang, M. García-Gabilondo, A. Grayston, I. V. J. Feiner, I. Anton-Sales, R. A. Loiola, J. Llop, P. Ramos-Cabrer, I. Barba, D. Garcia-Dorado, F. Gosselet, A. Rosell and A. Roig, *Nanoscale*, 2020, **12**, 4988–5002.

4 A. Grayston, Y. Zhang, M. Garcia-Gabilondo, M. Arrúe, A. Martin, P. Kopcansky, M. Timko, J. Kovac, O. Strbak, L. Castellote, S. Belloli, R. M. Moresco, M. Picchio, A. Roig and A. Rosell, *J. Cereb. Blood Flow Metab.*, 2022, **42**, 237–252.

5 S. Sathiensathaporn, A. Solé-Porta, D. Baowan, D. Pissuwan, P. Wongtrakoongate, A. Roig and K. P. Katewongsa, *J. Food Sci.*, 2025, **90**, e17631.

6 A. Areny-Balagueró, W. Mekseriwattana, M. Camprubí-Rimblas, A. Stephany, A. Roldan, A. Solé-Porta, A. Artigas, D. Closa and A. Roig, *Pharmaceutics*, 2022, **14**, 1447.

7 L. Nahidiazar, A. V. Agronskaia, J. Broertjes, B. Den Van Broek and K. Jalink, *PLoS One*, 2016, **11**, e0158884.

8 P. Delcanale and L. Albertazzi, *Data Br.*, 2020, **30**, 105468.

9 N. Feiner-Gracia, M. Beck, S. Pujals, S. Tosi, T. Mandal, C. Buske, M. Linden and L. Albertazzi, *Small*, 2017, **13**, 1701631.

10 S. H. Lee, J. Y. Shin, A. Lee and C. Bustamante, *Proc. Natl. Acad. Sci.*, 2012, **109**, 17436–17441.

11 D. Nino, N. Rafiei, Y. Wang, A. Zilman and J. N. Milstein, *Biophys. J.*, 2017, **112**, 1777–1785.